

# Pinning modes of high magnetic field Wigner solids with controlled alloy disorder

B.-H. Moon,<sup>1</sup> L. W. Engel,<sup>1</sup> D. C. Tsui,<sup>2</sup> L. N. Pfeiffer,<sup>2</sup> and K. W. West<sup>2</sup>

<sup>1</sup>*National High Magnetic Field Laboratory,  
1800 E. Paul Dirac Drive, Tallahassee, FL 32310*

<sup>2</sup>*Department of Electrical Engineering,  
Princeton University, Princeton, NJ 08544*

(Dated: May 4, 2021)

## Abstract

For a series of samples with 2D electron systems in dilute  $\text{Al}_x\text{Ga}_{1-x}\text{As}$ , with varying  $x$  from 0 to 0.8%, we survey the pinning mode resonances of Wigner solids at the low Landau filling termination of the fractional quantum Hall effect (FQHE) series. For all  $x$  studied, the pinning modes are present with frequencies,  $f_{\text{pk}}$ , that are consistent with collective weak pinning. For  $x \geq 0.22\%$  we find  $f_{\text{pk}}$  vs  $B$  exhibits a rapid increase that is not present for  $x = 0$ . We find the observed  $f_{\text{pk}}$  is much smaller than values calculated with a simple Wigner solid model which neglects the effects of the disorder on the charge distribution of a carrier.

In two-dimensional electron systems (2DES) hosted in GaAs an insulating phase occurs at the low Landau filling factor ( $\nu$ ) termination of the fractional quantum Hall effect (FQHE)<sup>1</sup> series. The insulator is understood as a form of Wigner solid<sup>2-14</sup>, a state of matter composed of charge carriers arranged to minimize their mutual repulsion while constrained to a fixed density by charge neutrality. The role of the disorder is crucial in producing the insulating behavior, since the Wigner solid is necessarily pinned by any disorder.

The spectra of the low  $\nu$  insulating phases of 2DES exhibit a microwave or rf resonance<sup>6-9,12,13</sup> that is identified as a pinning mode<sup>7,9,12-15</sup>, in which pieces of the solid oscillate collectively about their pinned positions. This disorder-induced mode is a powerful tool for study of solid phases in 2DES, which occur under many conditions<sup>14</sup> besides the low  $\nu$  insulator. But a detailed understanding of how the solid phase is pinned is lacking. The frequency,  $f_{pk}$ , of the resonance has been qualitatively found to increase with increasing accidental disorder, as roughly characterized by the mobilities of a variety of samples, but there is no systematic experimental knowledge of the relationship between the disorder characteristics and the pinning mode, and no microscopic picture of the solid in the presence of disorder.

This paper presents pinning mode measurements of the low  $\nu$  insulator in a series of samples with quantifiable, controlled alloy disorder, produced by using a dilute Al alloy,  $\text{Al}_x\text{Ga}_{1-x}\text{As}$ , as the channel in which the 2DES resides. The characteristics of these samples have been well established in earlier work on these wafers<sup>16-20</sup>. In particular, study<sup>16</sup> of the mobility vs  $x$  has shown that for  $x \leq 0.85\%$  the Al is randomly distributed in the channel, and has allowed modeling the potential around each Al atom as a spherical square well with known radius and potential-depth parameters. Relevant for high magnetic field ( $B$ ) studies, both this radius and the typical Al spacing in three dimensions are much less than the magnetic length,  $l_B$ , for all nonzero  $x$  that we studied, and for any accessible  $B$ . The samples we studied with  $x > 0$  had  $\sim 10^2$  to  $10^3$  Al within the typical volume of a carrier.

An important aspect of the disorder in 2DES in high  $B$  is its effect on the boundary between the insulating phase and fractional quantum Hall liquid states. The lowest disorder n-type 2DES in GaAs are insulating for  $\nu$  up to the 1/5 FQHE, and also have a narrow reentrant  $\nu$  range of insulating phase just above the 1/5 FQHE. Samples of somewhat larger disorder remain insulating up to the 1/3 FQHE<sup>21,22</sup>. One explanation of this is that the pinning energy, which allows the solid to reduce the charge near high points in the impurity

potential, can stabilize the Wigner solid<sup>23</sup> against transition to fractional quantum Hall liquids. Using samples from some of the same wafers studied in this paper, ref<sup>17</sup> describes how the phase boundary between the insulating phase and fractional quantum Hall liquid states is shifted to higher  $\nu$  by dilute Al alloy disorder, and demonstrates the terminal (lowest  $\nu$ ) FQHE is at  $1/3$  for  $x \geq 0.21\%$ . For the samples of Ref. 17, and in one other case<sup>22</sup>, a reentrant range of insulator in a narrow range of  $\nu$  above the  $1/3$  FQHE can be present.

We find that the resonance is clearly observable even at the largest  $x$  of  $0.85\%$ , at which  $f_{\text{pk}}$  is increased from its  $x = 0$  value by about one order of magnitude. Considering only the known densities of the samples, and using a classical shear modulus<sup>24</sup> the disorder-enhanced  $f_{\text{pk}}$  are consistent with the weak pinning picture<sup>25-28</sup>, in which the carrier positions are determined by a tradeoff between the disorder potential and the electron-electron interaction, and the disorder potential is not completely dominant. In the  $x > 0$  samples  $f_{\text{pk}}$  increases rapidly as  $\nu$  decreases into the insulating phase, in rough agreement with the theories. We estimate the parameters of the disorder in a simple model that takes a carrier of the lattice to have the fixed charge distribution of a lowest Landau level orbital. Using these disorder parameters in weak pinning theories<sup>26,28</sup> overestimates the effect of the alloy disorder, and predicts that pinning resonances, if present at all, would be at much higher frequency than we observed. This discrepancy could be resolved by the charge distribution at a carrier in the disordered samples responding in a way that reduces pinning energy.

The form of transmission-line-based<sup>6</sup> broadband microwave spectroscopy technique we use has been described elsewhere<sup>14,29</sup>. We calculated the real part of diagonal conductivity,  $\text{Re}(\sigma_{xx})$ , from the loss on transmission line patterned in metal film directly on the sample surface, about 180 nm above the 2DES. The transmission is of coplanar waveguide type, as is shown schematically in Figure 1a. We used a room-temperature transmitter and receiver to measure the transmitted power,  $P$ , and present data calculated from  $\text{Re}(\sigma_{xx}) \approx -W |\ln(P/P_0)| / 2Z_0d$  where  $W = 30 \mu\text{m}$  is the slot width between center line and ground plane of the coplanar waveguide,  $P_0$  is the reference power obtained from an average of transmitted power at  $\nu = 1$  and  $2$ .  $Z_0 = 50 \Omega$  is the characteristic impedance calculated from the transmission line geometry for  $\sigma_{xx} = 0$ , and  $d$  is the length of the line ( $d = 28$  mm). The formula is a low loss, high frequency approximation valid to within about 20%, from comparison with a detailed calculation, like that described in Ref. 29, including the distributed capacitive coupling and allowing for higher loss and reflection. We estimate the

2DES temperature to be approximately 50 mK, as read by nearby resistance thermometers. Slight broadening of the resonance could be discerned on increasing the temperature above that value. The data are taken in the low microwave power limit, in which further decrease of power (at all frequencies measured, and at 50 mK) does not affect the measurement.

In the samples we studied the 2DES is confined at a single  $\text{Al}_{x_s}\text{Ga}_{1-x_s}\text{As} / \text{Al}_x\text{Ga}_{1-x}\text{As}$  heterojunction, where  $x = 0, 0.21, 0.33, 0.4, 0.8$  or  $0.85\%$  for the layer in which the 2DES mainly resides, and  $x_s \gg x$  is the Al concentration of the spacer layer. Table I shows typical densities ( $n$ ) for the microwave measurements, and low temperature mobilities from different pieces of the same wafers<sup>16,30</sup>, scaled<sup>31</sup> to the densities shown. The samples were grown in two series with different characteristics<sup>30</sup>; series 1 includes  $x = 0, 0.21, 0.33$  and  $0.85\%$  with  $x_s = 30\%$ , and series 2 includes  $x = 0.4$  and  $0.8\%$  with  $x_s = 10\%$ . There is other disorder present in addition to that due to the Al in the channel. This background disorder arises from the potential from remote ionized donors, alloy disorder in the spacer, interface roughness and accidental impurities introduced throughout the growth; this background disorder is what gives rise to the pinning mode in the  $x = 0$  sample. The mobilities in Table 1 clearly show a larger background disorder for series 1; for example the  $x = 0.4\%$  sample of series 2 has higher mobility than lower  $x$  samples in the series 1. Various densities,  $n$ , were prepared by brief low temperature illumination before the measurements.

$x$ (%)	Wafer Name	$\mu$ ( $10^6 \text{ cm}^2/\text{V-s}$ )	$n$ ( $10^{10} \text{ cm}^{-2}$ )
0	7-30-97-2	2.0	4.6
0.21	8-21-97-2	2.3	5.9
0.33	8-06-97-1	1.7	5.6
0.40	12-03-04-1	2.6	4.9
0.80	12-06-04-1	1.6	4.9
0.85	7-30-97-2	0.72	8.2

TABLE I: Sample parameters, including Al fraction ( $x$ ) for the layer in which the 2DES mainly resides, mobility ( $\mu$ ) and areal density  $n$ .

Figure 1b shows  $\text{Re}(\sigma_{xx})$  vs  $B$  at 1, 5 and 8 GHz, for the sample with  $x = 0.8\%$ . Dips at  $\nu = 1/3$  and  $2/5$  are clearly visible confirming the finding<sup>17</sup> that the alloy disorder does not

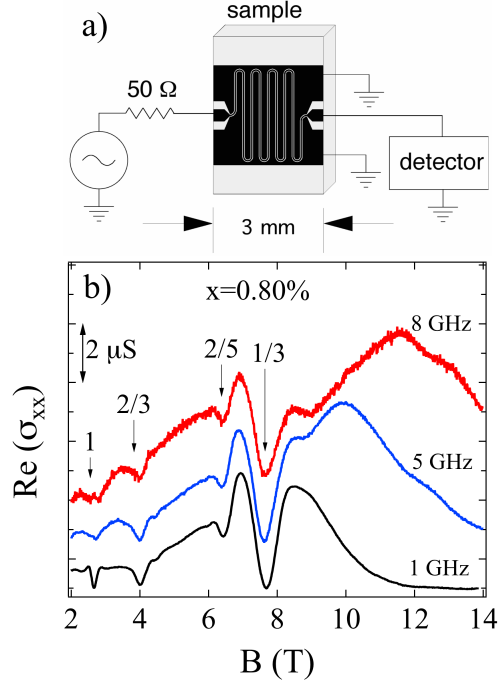


FIG. 1: a) Schematic representation of the microwave circuit used in our measurement, not to scale. Black areas represent metal films on the sample surface. b) Real diagonal conductivity,  $\text{Re}(\sigma_{xx})$ , vs magnetic field,  $B$ , for Al fraction  $x = 0.8\%$ , density  $n = 6.2 \times 10^{10} \text{ cm}^{-2}$  at three different frequencies.

inhibit formation of these FQHE states. FQHE features are present for the lower  $x$  samples as well. In the figure there is slight decrease of  $n$ , of about 3% as  $B$  increases to 8 T, and the  $\nu$  marked on the figure are taken from the  $1/3$  FQHE minimum.  $\nu$  is calculated from that minimum for all data presented in this paper. As  $\nu$  goes below  $1/3$ , the 5 and 8 GHz traces increase markedly owing to the onset of the pinning resonance. Reference 17 reported a reentrant insulating phase for  $\nu$  between the  $1/3$  and  $2/5$  FQHE's for an Al alloyed sample with  $x = 0.85\%$  and much larger  $n$ ; the data in Figure 1b show no sign of a resonance in that  $\nu$  range.

Figure 2 shows spectra taken at many  $\nu$  for the samples with  $x = 0, 0.21, 0.4$  and  $0.8\%$ . For  $x = 0$ , at  $n = 4.6 \times 10^{10} \text{ cm}^{-2}$ , the resonance emerges as  $\nu$  is decreased below  $1/3$ , growing sharper and developing large peak conductivity as  $\nu$  is decreased further. The resonance appears superposed on a smaller, decreasing smooth background, which is an artifact of the normalization power  $P_0$ .  $P_0$ , an average of measurements taken at integer

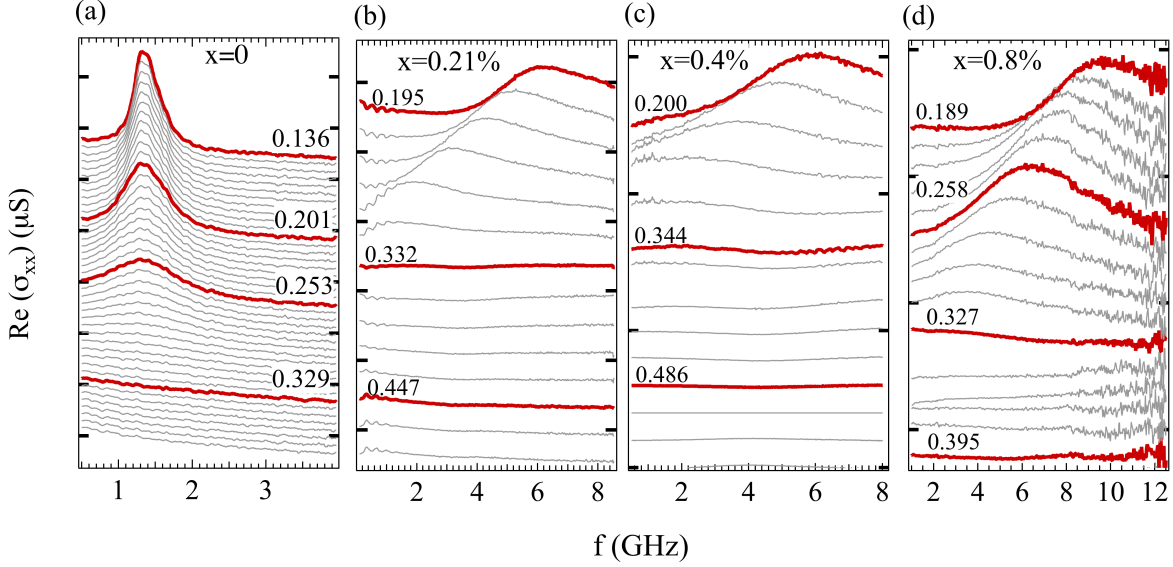


FIG. 2: Spectra, real diagonal conductivity  $\text{Re}(\sigma_{xx})$  vs frequency,  $f$ , offset vertically for successively lower Landau fillings,  $\nu$ .  $\nu$  for heavy (red online) lines is marked on graphs. Tick marks on the vertical axes are separated by  $10 \mu\text{S}$ . a) Al fraction  $x = 0$ , density  $n = 4.6 \times 10^{10} \text{ cm}^{-2}$ . Successive traces were taken at  $\nu$  decremented by  $\Delta\nu = 0.0065$ , b)  $x = 0.21\%$ ,  $n = 8.0 \times 10^{10} \text{ cm}^{-2}$ ,  $\Delta\nu = 0.0058$ . c)  $x = 0.40\%$ ,  $n = 6.7 \times 10^{10} \text{ cm}^{-2}$ ,  $\Delta\nu = 0.029$ . d)  $x = 0.80\%$ ,  $n = 6.2 \times 10^{10} \text{ cm}^{-2}$ ,  $\Delta\nu = 0.0137$ .

$\nu$ , had a component that decreased with  $f$ , which we ascribe to parallel conduction. The background has no significance for our results.

A resonance is clearly present for the samples with  $x > 0$ , as shown in Figure 2b, c and d. As in the  $x = 0$  sample of Figure 2a, the resonance develops as  $\nu$  is decreased below  $1/3$ . For all the samples with  $x > 0$ , the resonance frequency shifts upwards as  $\nu$  decreases.

Figure 3a shows  $f_{\text{pk}}$  vs  $\nu$  for all the samples.  $f_{\text{pk}}$  for  $x = 0$  can be regarded as a background, and is much smaller than the  $f_{\text{pk}}$  for other curves, except where the resonance is quite weak, near the low- $\nu$  edge of the  $1/3$  FQHE. This means that for the well-developed resonances with  $x > 0$ , the Al dilute alloy is the main contribution to the pinning frequency. For  $0.2 \leq x \leq 0.4\%$  there is little variation in  $f_{\text{pk}}$  vs  $\nu$  for the several  $n$  values presented. However, on increasing  $x$  to  $0.8\%$  there is again a definite increase in  $f_{\text{pk}}$ . The relatively small change of  $f_{\text{pk}}$  between  $x = 0.2$  and  $0.4\%$  may be explainable by background disorder, contributed by other sources than the deliberately introduced Al. Except for the 0.21 and

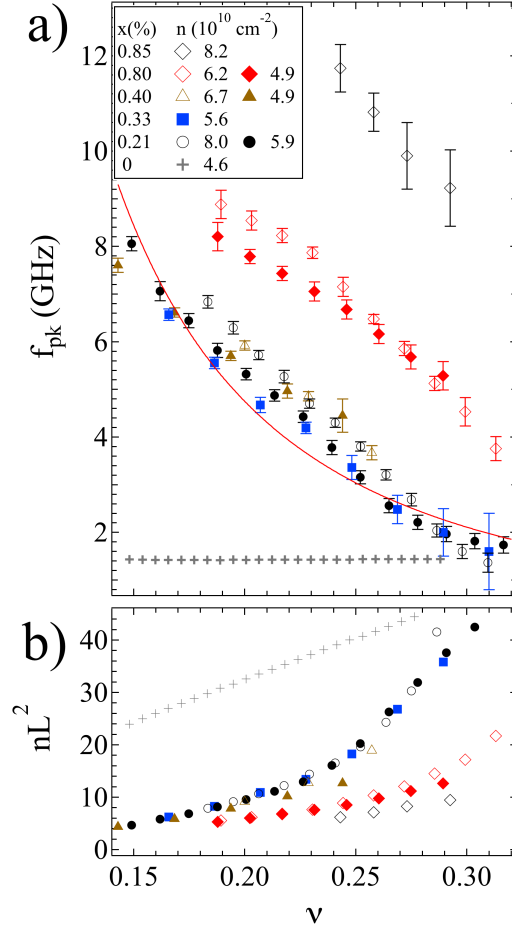


FIG. 3: a) Resonance peak frequency,  $f_{pk}$ , vs Landau filling,  $\nu$ , for various Al alloy fractions  $x$  and densities  $n$ , as marked in the legend. Thin curve is  $f_{pk} = 0.19/\nu^2$ . b) Number of carriers per domain vs  $\nu$ , symbols same as in a.

0.33% samples of series 1, whose resonance frequencies are close together,  $f_{pk}$  at any  $\nu$  increases with  $x$  within each series.

In the collective pinning case, the solid deformation occurs over a large enough length that deformation energy can be calculated from the shear modulus  $\mu_s$ . Theories<sup>25–28</sup> for the collective pinning case connect a correlation length of the crystalline order to  $f_{pk}$  independent of other characteristics of the disorder, as  $L = (\mu_s \pi / 2neBf_{pk})^{1/2}$ . For collective pinning to apply,  $nL^2 \gg 1$  is required. As a rough estimate we take  $\mu_s$  to be the classical value for point particles in a triangular lattice<sup>24</sup>  $\mu_{cl} = 0.245e^2 / 4\pi\epsilon\epsilon_0 n^{3/2}$ . Calculations<sup>3,4,32</sup> that take quantum effects into account using the composite fermion picture give values of  $\mu_s$  that are about 30% larger than  $\mu_{cl}$  for the relevant range of  $\nu$ . Figure 3b shows the the number of

carriers per domain ( $nL^2$ ) vs  $\nu$ , with  $L$  calculated in this way using  $\mu_{cl}(n)$ . Particularly for larger  $\nu$ , including conditions under which the resonance is well developed, the collective pinning condition  $nL^2 \gg 1$  is satisfied.

A semiclassical picture<sup>26-28</sup> was developed to explain high magnetic field Wigner solid pinning in weak disorder with correlation length smaller than  $l_B$ . In the semiclassical model the carrier guiding centers move in an “effective potential” that results from convolving the true impurity potential with the charge distribution “form factor” of a carrier. Using the notation of Ref. 28, the true impurity potential is characterized by its correlation length  $\xi$  and its variance  $C(0)$ . The charge distribution of each carrier is taken from single particle lowest Landau level orbitals in symmetric gauge, a Gaussian of characteristic radius  $l_B$ . In the case  $\xi \ll l_B$ , which would hold true for the Al alloyed samples considered here, the effective potential (resulting from the convolution) has correlation length  $l_B$  and variance  $C(0)\xi^2/l_B^2$ . Minimizing the total of deformation and pinning energies gives

$$L = \frac{\mu_s l_B^3 (2\pi)^{1/2}}{n^{1/2} \xi C(0)^{1/2}}, \quad f_{pk} = \frac{C_0 \xi^2}{4eB\mu_s l_B^6}. \quad (1)$$

The theories<sup>26,28</sup> predict that  $f_{pk} \propto \nu^{-2}$  for collective pinning with the  $\xi \ll l_B$ . A curve of  $f_{pk} \propto \nu^{-2}$  is superposed on the data in Figure 3a. While the data are clearly not a fit to  $f_{pk} \propto \nu^{-2}$ , the relation roughly describes the extent of the change of  $f_{pk}$  over the experimental range of  $\nu$ . The discrepancy between the data and  $f_{pk} \propto \nu^{-2}$  may be due to an increase  $\mu_s$  as  $\nu$  decreases. Such variation of  $\mu_s$  vs  $\nu$  has been predicted<sup>3,32</sup>, using theory based on composite fermion Wigner solids. The change of  $f_{pk}$  with  $\nu$  in Figure 3a is in contrast with the essentially flat  $f_{pk}$  vs  $\nu$  for  $x = 0$ , and is an effect of the alloy disorder. In other work, moderate mobility samples without deliberately induced disorder<sup>12,13,33</sup> have  $f_{pk}$  vs  $\nu^{-1}$  increasing sublinearly as  $\nu$  enters the insulating phase or exhibiting a shallow maximum<sup>12</sup>.

It is of interest to try to apply the known parameters of the alloy disorder potential to the semiclassical weak pinning calculations. In this picture, the energy due to each Al in contact with the carrier is  $E_{Al} = v_{Al}\mathcal{E}/2\pi l_B^2 z_0$ , where  $v_{Al} = 6.16 \times 10^{-29} \text{m}^{-3}$ ,  $\mathcal{E} = 1.3 \text{ eV}$  are the volume and depth of the spherical square well from Ref. 16, and  $2\pi l_B^2 z_0$  is an effective volume of the carrier. Thickness  $z_0$  is estimated from the Fang-Howard wave function<sup>34</sup> at the sample density,  $n$ . Defining  $n_{i3d}$  as the density of the dilute Al,  $n_{i3d} = x/v_0$ , where  $v_0$



is the unit cell volume of the  $\text{Al}_x\text{Ga}_{1-x}\text{As}$ , there are an average of  $N_{\text{Al}} = 2\pi l_B^2 z_0 n_{\text{3d}}$  Al per carrier.  $N_{\text{Al}} \approx 10^3$  and total pinning energy per carrier due to Al is  $E_{\text{Al}} N_{\text{Al}} / k_B \approx 140$  K. With randomly distributed Al, the variance,  $V_L^2$ , of the pinning energy of a domain (area  $L^2$ ) is  $E_{\text{Al}}^2 N_{\text{Al}} n L^2$ . Energy is minimized by setting  $V_L = \mu_s \delta^2$ , where  $\delta$  is the displacement required to randomize the carrier pinning energy. Taking  $\delta = l_B$  obtains equations (1) for  $L$  and  $f_{\text{pk}}$  with  $C(0)\xi^2$  substituted by  $\mathcal{E}^2 v_{\text{Al}}^2 n_{\text{3d}} / z_0$ .

The results of this calculation, however, are not consistent with the observation of a microwave-range resonance in the  $x > 0$  samples. The calculated  $f_{\text{pk}}$  is about three orders of magnitude too large for any of the resonances shown in this paper, and the calculated  $L$  would be much less than  $l_B$ . The pinning energy per Landau orbital carrier is about half the cyclotron energy for the largest  $x$  of 0.8% and  $B = 14$  T. It is possible that the carrier wave function is affected by disorder, so that the Landau orbital is a poor approximation. With random short-range disorder a more spread-out charge distribution would produce weaker pinning. In equations 1 this larger effective carrier size could be modeled by substituting  $l_B$  with a larger length. Correlations between carriers, such those incorporated in the composite fermion picture<sup>3</sup> are also likely to be of importance. A more complete picture of a disorder pinned state including correlations was considered by Yannouleas and Landmann<sup>35</sup>. They found that larger disorder produces pinned charge-density-wave-like states with reduced charge modulation amplitude, compared with that of Wigner crystals in the low disorder case.

In summary, we have found well-developed microwave resonances in 2DES hosted in dilute  $\text{Al}_x\text{Ga}_{1-x}\text{As}$ , in the solid at the low  $\nu$  termination of the FQHE series, for  $x$  up to 0.8%. Relative to the  $x = 0$  case, the Al significantly increases  $f_{\text{pk}}$  and also causes a much stronger increase of  $f_{\text{pk}}$  as  $\nu$  decreases into the range of the solid phase. Semiclassical theory for the case of weak disorder, in which a carrier is taken as having a lowest Landau level single-particle form, is not adequate to explain the observation of the pinning modes in the Al alloyed samples.

We thank Kun Yang and J. K. Jain for helpful discussions. The work at Princeton was partially funded by the Gordon and Betty Moore Foundation and the NSF MRSEC Program through the Princeton Center for Complex Materials (DMR-0819860). The microwave spectroscopy work at NHMFL was supported through DOE grant DE-FG02-05-ER46212 at NHMFL/FSU. NHMFL is supported by NSF Cooperative Agreement No. DMR-0084173,

the State of Florida and the DOE.

---

- <sup>1</sup> D. C. Tsui, H. L. Stormer, and A. C. Gossard Phys. Rev. Lett. **48**, 1559 (1982).
- <sup>2</sup> Y. E. Lozovik and V. I. Yudson, JETP Lett., **22**, 11 (1975); P. K. Lam and S. M. Girvin, Phys. Rev. **B 30**, 473 (1984); Kun Yang, F. D. M. Haldane, and E. H. Rezayi Phys. Rev. B **64**, 081301 (2001).
- <sup>3</sup> A. C. Archer, Kwon Park, Jainendra K. Jain, Phys. Rev. Lett., **111**, 146804 (2013).
- <sup>4</sup> Chia-Chen Chang, Csaba Töke, Gun Sang Jeon, and Jainendra K. Jain Phys. Rev. B **73**, 155323 (2006); Chia-Chen Chang, Gun Sang Jeon, and Jainendra K. Jain Phys. Rev. Lett. **94**, 016809 (2005).
- <sup>5</sup> M. Shayegan, in Perspectives in Quantum Hall Effects, edited by S. Das Sarma and A. Pinczuk (Wiley-Interscience, New York, 1997), p. 343.
- <sup>6</sup> E. Y. Andrei, G. Deville, D. C. Glattli, F. I. B. Williams. E. Paris, and B. Etienne, “Observation of a magnetically induced Wigner solid,” Phys. Rev. Lett. **60**, 2765 (1988).
- <sup>7</sup> F. I. B. Williams, P. A. Wright, R. G. Clark, E. Y. Andrei, G. Deville, D. C. Glattli, O. Probst, B. Etienne, C. Dorin, C. T. Foxon, and J. J. Harris Phys. Rev. Lett. **66**, 3285 (1991).
- <sup>8</sup> M. A. Paalanen, R. L. Willett, R. R. Ruel, P. B. Littlewood, K. W. West, L. N. Pfeiffer and D. J. Bishop, Phys. Rev. B **45**, 11342 (1992).
- <sup>9</sup> M. A. Paalanen, R. L. Willett, R. R. Ruel, P. B. Littlewood, K. W. West, L. N. Pfeiffer and D. J. Bishop, Phys. Rev. B **45**, 13784 (1992).
- <sup>10</sup> H. Buhmann, W. Joss, K. v. Klitzing, I. V. Kukushkin, A. S. Plaut, G. Martinez, K. Ploog, and V. B. Timofeev, Phys. Rev. Lett. **66**, 926 (1991).
- <sup>11</sup> I. V. Kukushkin, Vladimir I. Falko, R. J. Haug, K. von Klitzing, K. Eberl, and K. Ttemayer Phys. Rev. Lett. **72**, 3594(1994).
- <sup>12</sup> P. D. Ye, L. W. Engel, D. C. Tsui, R. M. Lewis, L. N. Pfeiffer, and K. West, Phys. Rev. Lett. **89**, 176802 (2002).
- <sup>13</sup> L. W. Engel ,C.-C. Li, D. Shahar, D. C. Tsui and M. Shayegan, Solid State Commun., **104** 167-171 (1997).
- <sup>14</sup> G. Sambandamurthy, Zhihai Wang, R.M. Lewis, Yong P. Chen, L.W. Engel, D.C. Tsui, L.N. Pfeiffer and K.W. West, Solid State Commun. **140**, 100 (2006) contains a brief review.

- <sup>15</sup> Hidetoshi Fukuyama and Patrick A. Lee Phys. Rev. B **18**, 6245 (1978).
- <sup>16</sup> Wanli Li, G.A. Csáthy, D.C. Tsui, L.N. Pfeiffer, and K.W. West, Appl. Phys. Lett. **83**, 2832 (2003).
- <sup>17</sup> Wanli Li, D. R. Luhman, D. C. Tsui, L. N. Pfeiffer, and K. W. West Phys. Rev. Lett. **105**, 076803 (2010).
- <sup>18</sup> Wanli Li, G.A. Csáthy, D. C. Tsui, L. N. Pfeiffer, and K. W. West Phys. Rev. Lett. **94**, 206807 (2005).
- <sup>19</sup> Wanli Li, C. L. Vicente, J. S. Xia, W. Pan, D. C. Tsui, L. N. Pfeiffer, and K. W. West Phys. Rev. Lett. **102**, 216801 (2009).
- <sup>20</sup> Wanli Li, J. S. Xia, C. Vicente, N. S. Sullivan, W. Pan, D. C. Tsui, L. N. Pfeiffer, and K. W. West Phys. Rev. B **81**, 033305 (2010).
- <sup>21</sup> D. Shahar, D. C. Tsui, M. Shayegan, R. N. Bhatt and J. E. Cunningham, Phys. Rev. Lett. **74**, 4511 (1995).
- <sup>22</sup> I. Yang, W. Kang, S. T. Hannahs, L.N. Pfeiffer, and K.W. West, Phys. Rev. B **68**, 121302(R) (2003).
- <sup>23</sup> R. Price, Xuejun Zhu, P. M. Platzman, and Steven G. Louie Phys. Rev. B **48**, 11473 (1993).
- <sup>24</sup> L. Bonsall and A. A. Maradudin Phys. Rev. B **15**, 1959 (1977).
- <sup>25</sup> H. Fukuyama, and P. A. Lee, Phys. Rev. B **18**, 6245 (1978).
- <sup>26</sup> R. Chitra, T. Giamarchi, and P. Le Doussal, Phys. Rev. Lett. **80**, 3827 (1998); R. Chitra, T. Giamarchi, and P. Le Doussal, Phys. Rev. B **65**, 035312 (2001).
- <sup>27</sup> H. A. Fertig, Phys. Rev. B **59**, 2120 (1999).
- <sup>28</sup> M. M. Fogler, and D. A. Huse, Phys. Rev. B **62**, 7553 (2000).
- <sup>29</sup> Zhihai Wang, Yong P. Chen, Han Zhu, L. W. Engel, D. C. Tsui, E. Tutuc, and M. Shayegan Phys. Rev. B **85**, 195408 (2012).
- <sup>30</sup> Wanli Li, doctoral dissertation, Princeton University, 2007.
- <sup>31</sup> Loren Pfeiffer, K. W. West, H. L. Stormer, and K. W. Baldwin Appl. Phys. Lett. **55**, 1888 (1989).
- <sup>32</sup> R. Narevich, Ganpathy Murthy, and H. A. Fertig Phys. Rev. B **64**, 245326 (2001).
- <sup>33</sup> C.-C. Li, L. W. Engel, D. Shahar, D. C. Tsui, and M. Shayegan Phys. Rev. Lett. **79**, 1353(1997).
- <sup>34</sup> F.F. Fang and W. E. Howard, Phys. Rev. Lett. **16**, 797 (1966). We use  $z_0 = 3(8\hbar^2\epsilon\epsilon_0/33m^*e^2n)^{1/3}$ , where  $m^*$  is the band mass. For the 2DES studied here,  $n$  was between

4.9 and  $8 \times 10^{10} \text{ cm}^{-2}$ , from which the calculated  $z_0$  was between 22 and 19 nm.

<sup>35</sup> C. Yannouleas and U. Landman, Phys. Rev. B **84**, 165327 (2011).